JOURNAL OF CATALYSIS **159,** 90–98 (1996)
ARTICLE NO. 0067

Methylcyclopentane Conversion Catalysis over Zeolite-Y Encaged Rhodium: A Test for the Metal–Proton Adduct Model

T. J. McCarthy, G.-D. Lei, and W. M. H. Sachtler[1]

V. N. Ipatieff Laboratory, Center for Catalysis and Surface Science, Department of Chemistry, Northwestern University, Evanston, Illinois 60208

Received July 28, 1995; revised October 30, 1995; accepted October 31, 1995

The conversion of methylcyclopentane (MCP) has been studied over zeolite Y supported rhodium catalysts with a variety of proton concentrations. Ring opening (RO) of MCP to hexane isomers is catalyzed by metal sites, but ring enlargement (RE) of MCP to cyclohexane and benzene requires metal sites and acid protons. The activity for RE of Rh/HY is 2.5 times higher than that of physical mixtures of neutralized $Rh/NaY_{(neutr)}$ and HY with the same number of metal and acid sites at 200°C. This illustrates the importance of proximity between metal and acid sites and suggests that rhodium–proton adducts, $[Rh_nH_x]^{x+}$, behave as *collapsed bifunctional sites*. Initial overall activity at 200°C decreases with increasing proton concentration in the order Rh/SiO_2 > $Rh/NaY_{(neutr)}$ > Rh/NaY > Rh/HY. In contrast to RE, the intrinsic activity of rhodium–proton adducts for RO is much lower than that of proton-free Rh clusters. This difference is not caused by preferential site blocking with coke precursors, as follows from temperature-programmed oxidation of the catalyst after MCP reaction. Likewise, cyclopentane H/D exchange, a reaction that specifically probes for uncovered metal sites, shows that the free metal surface in Rh/HY decreases only by 25% upon exposure to MCP. Since the activity differences between Rh/HY and Rh/NaY cannot be attributed to different metal coverages with carbonaceous deposits, it follows that the decrease in RO activity with increasing proton concentration of the zeolite results from coverage of metal sites with carbenium ions, which is a direct consequence of metal–proton adduct formation. © 1996 Academic Press, Inc.

I. INTRODUCTION

In the present study, theoretical models for bifunctional catalysis are tested by exploiting the extraordinarily high activity of rhodium for hydrogenolysis of hydrocarbons. The term *bifunctional catalyst* stands for a heterogeneous catalyst that exposes two types of active sites, e.g., acid sites and ensembles of transition metals. Well known examples are those catalysts used in catalytic reforming that expose Pt and acid sites.

In the classical model of bifunctional catalysis, proposed by Mills *et al.* (1), isomerization of an *n*-alkane is assumed to start with the adsorption of the feed molecule on a metal site, where it is dehydrogenated to an olefin. This can move to an acid site, where it is adsorbed as a secondary carbenium ion which can isomerize to a tertiary carbenium ion. When this species decomposes into a surface proton and a branched olefin, that molecule is adsorbed at a metal site, where it is hydrogenated to a branched alkane molecule.

In our previous work with zeolite supported transition metals, we obtained evidence that zeolite protons and metal clusters can interact to form a "metal–proton adduct" (2). These adducts are able to act as "collapsed bifunctional sites." Alkane isomerization can be visualized taking place on such sites without the need of the intermediates to "shuttle" between metal and acid sites, as all reaction steps can be realized during one single residence of the molecule. No endothermic decomposition of adsorbed carbenium ions into protons and desorbed olefin molecules is required in this model; hydride ion transfer from an impinging or physisorbed alkane to an adsorbed carbenium ion transforms the latter to a product molecule. Evidence was obtained that bifunctional reactions catalyzed by metal–proton adducts are more rapid than those catalyzed by physically separated metal and acidic sites (2).

A second beneficial effect of the formation of metal–proton adducts is that the protons of these complexes act as anchors for the metal clusters. As a consequence, agglomeration of metal clusters to larger particles is impeded, i.e., a high metal dispersion is maintained (3–5) while its propensity to strongly chemisorb hydrogen is reduced (6). The high dispersion maintenance, occurring even under rather severe conditions, proves that the metal–proton adducts are fairly stable.

It has also been proposed that charge sharing between metal clusters and surface protons is assumed to render the metal electron deficient (7–9). Boudart and co-workers reported the turnover frequency of neopentane hydrogenolysis at 272°C to be 44 times higher for Pt/CaY than for Pt/Al_2O_3. They attribute this enhanced activity to a partial electron transfer from the small Pt particles to the zeolite support (10, 11). The electronic state of the metal can be modified such that the metal particles become electron

[1] To whom correspondence should be addressed.

0021-9517/96 $18.00

rich as in the case of alkaline Pt/L zeolites (12–14). It has been shown by *ab initio* calculations carried out on the $[PdCl(H)Me_2(NH_3)\cdots NH_3]$ and $[PdCl(Me)_2(NH_3)\cdots H–NH_3]$ model system that the Pd(IV)hydride complex is less stable than the corresponding $Pd(II)\cdots H–N$ tautomer. The $Pd^{n+}\cdots H–N$ complexes are similar to $Pd\cdots H–O_{zeolite}$ adducts (15). Direct IR evidence for the chemical interaction of acid protons and transition metal ions has been reported for intermolecular $M\cdots H–O$ hydrogen-bonding between $Cp^*M(CO)_2$ ($M=$ Co, Rh, Ir) and a number of fluoro alcohols (16).

The objective of the present study is to explore the catalytic potential of $[Rh_nH_x]^{x+}$ adducts with the methylcyclopentane (MCP) probe reaction. It is well known that MCP can undergo two types of reactions:

(i) Ring opening (RO), i.e., hydrogenolytic conversion into the three isomeric hexane molecules. This reaction is catalyzed by all transition metals, rhodium being the most active.

(ii) Ring enlargement (RE), i.e., a six-C-ring molecule is formed, which is desorbed either as cyclohexane or as benzene, depending on the hydrogen pressure. This is a bifunctional reaction, requiring a metal and an acid site. The hypothesis that metals can also catalyze ring enlargement reactions via sequential ring opening and ring closure steps is discarded in these systems because there is no evidence of formation of ring enlargement products on any of the monofunctional metal/zeolite Y catalysts (2, 7).

In order to discriminate between the two models under discussion for bifunctional catalysts,

(a) geometrically separated acid and metal sites, and
(b) metal–proton adducts (collapsed bifunctional sites),

it will be useful to address the question of how catalysis will change upon lowering the temperature such that carbenium ions are still formed on acid sites, but with their isomerization and desorption (for instance by hydride ion transfer) being very slow.

For this situation both models predict a low rate of bifunctional catalysis, but for reactions which are solely catalyzed by the metal, model (a) predicts that such reactions will continue to proceed with the same rate as on a monofunctional catalyst that does not expose acid sites. In contrast, model (b) predicts that carbenium ions will block the metal sites: consequently the rate of purely metal-catalyzed reactions will be significantly lower than on a monofunctional catalyst at the same temperature.

Studying the catalytic selectivity at low temperature should therefore provide the means to discriminate between both models. This is the primary objective of the present study. Rhodium was chosen because its high activity for metal-catalyzed reactions permits data collection at lower temperatures than most other metals (17–20). Previous results indicate that protons modify the chemistry of zeolite supported rhodium clusters in zeolite Y (21). The rate of catalytic neopentane hydrogenolysis was found to be higher and the activation energy lower for catalysts containing both Rh clusters and protons than for proton-free samples, lending further credence to the rhodium–proton adduct concept (22).

An important question emerging from this research is what will happen at low temperatures, where the metal-catalyzed RO reaction is fast on rhodium but the bifunctionally catalyzed RE reaction with higher activation energy is very slow. This question will be addressed with reaction studies, temperature-programmed oxidation (TPO), and isotope exchange experiments.

II. EXPERIMENTAL

1. Sample Preparation and Pretreatment

The NaY and NH_4Y zeolite supports were prepared from LZ Y-52 (Si/Al = 2.6, Linde Molecular Sieves, Lot No. 968087061020-S-8). Two successive exchanges with a 20 molar excess of $NaNO_3$ at room temperature were performed to yield NaY. NH_4Y (90% exchange) was prepared by three successive exchanges having a 10 molar excess of NH_4Cl (solution temp. = 80°C). Rhodium was ion-exchanged into each support to achieve a weight loading of 3% Rh/NaY and 3% Rh/NH_4Y. A typical procedure involved slowly adding a dilute solution of $[Rh(NH_3)_5Cl]Cl_2$ (0.003 *M*) to a rapidly stirred zeolite slurry (3 g/liter, 80°C) over a 12 h period, followed by additional stirring for 60 h. The $[Rh(NH_3)_5Cl]Cl_2$ complex was obtained by reaction of $RhCl_3\cdot 2H_2O$ with NH_4OH solution, as described in the literature (23). After drying in air at room temperature, the metal loading was determined by ICP elemental analysis. The pretreatment conditions were selected on the basis of our previous experience (21).

Neutralization of the protons formed during the reduction of the Rh ions in the Rh/NaY sample was performed. The reduced catalyst was slurried in doubly distilled water (200 ml/g). The pH of the resultant slurry was adjusted to pH 10–11 by slow, dropwise addition of dilute NaOH. The sample was filtered, washed, and dried at room temperature in air. An FT-IR spectrum of the self supporting wafer was measured to confirm the removal of all O–H groups.

The 5% Rh/SiO_2 sample was prepared by a conventional impregnation technique described elsewhere (24). The Rh source was $RhCl_3\cdot 2H_2O$ (Johnson/Matthey). After impregnation, the catalyst was dried in air and then at 110°C for 3 h.

Calcinations were carried out in an O_2 flow (UHP, Linde; 140 ml/min) while the temperature was ramped at 0.5°C/min to 500°C, then held at the respective temperature for 2 h. The oxygen was purified by passing it over Pt/SiO_2 and a 4A molecular sieve. At the calcination tempera-

ture, the carrier gas was switched to He (High Purity Linde; 60 ml/min). The samples were held at that temperature under He for 20 min and then cooled to room temperature. Prior to reaction, the samples were heated to 400°C in H_2 (UHP, Linde; 30 ml/min.) at 8°C/min and then held at that temperature for 20 min. The hydrogen and helium were purified by passing them over MnO/SiO_2 and a 4A molecular sieve. The samples were then cooled to T_{rxn} under H_2 then switched to He prior to reaction.

2. Methylcyclopentane (MCP) Conversion

Methylcyclopentane was purchased from Fluka and further purified over a 5A molecular sieve. The MCP reaction was carried out on 100–200 mg of catalyst in a continuous flow microreactor under atmospheric pressure with a H_2/MCP ratio of about 18 (25). The reaction mixtures were obtained by passing the purified H_2 through an MCP saturator cooled to 0°C ($P_{MCP} = 0.0526$ atm) by a circulator (Polyscience) filled with a 50/50 mixture of ethylene glycol and water. The flow rates were held constant at 20 ml/min. Reaction products were analyzed by an on-line HP 5890 Series II gas chromatograph with a 50-m crosslinked methylsilicone fused capillary column equipped with a FID detector.

The site time yields (STY) reported in this paper are expressed as numbers of MCP molecules converted per reduced surface rhodium atom per second. For low conversion (<15%), the site time yield is equal to the turnover frequency (TOF). The number of reduced surface Rh atoms is obtained from a combination of H_2-TPR, H_2-TPD, EXAFS, and TEM results, as outlined by Tomczak *et al.* (21). The initial dispersions are Rh/SiO_2 (0.30), $Rh/NaY_{(neutr)}$ (0.62), Rh/NaY (0.63), and Rh/HY (0.79). These numbers are corrected for the amount of Rh^+ found in the Rh/NaY and Rh/HY catalysts.

3. Temperature-Programmed Oxidation (TPO)

Temperature programmed oxidation was performed on selected catalysts after MCP reactions in order to determine the amount of carbonaceous deposits. The system is described elsewhere (26). It uses an on-line mass spectrometer as a detector, allowing for simultaneous *in situ* analysis of oxygen consumption and product formation. After reaction to the specified times, the catalysts were cooled in flowing He (60 ml/min), sealed, and transferred to the TPO system. After purging in He, the samples were heated with a temperature ramp of 8°C/min from 25 to 650°C in a 5% O_2/5% Ar/He flow (30 ml/min). In all cases the rate of O_2 consumption mirrors the rate of CO_2 evolution. The C/Rh ratios were calculated, assuming a complete oxidation of the coke to CO_2 and using the total amount of exposed Rh^0 in the catalyst. This assumption was confirmed by monitoring the CO and CO_2 signals; their ratio was found to be of the order predicted by the Boudouard equilibrium.

4. Cyclopentane H/D Exchange

Exchange measurements were performed in a recirculation flow system, as described previously (27). The isotope exchange was monitored by a mass spectrometer (Dycor M100) with a variable leak valve from the reaction system. All samples (3 wt%) were calcined at 500°C and reduced at 400°C. All exchange reactions were carried out at 100°C with a deuterium to cyclopentane ratio of 25 and a total pressure of 52 Torr. The exchange rate was measured after reduction and then after exposure to H_2/MCP (ratio = 20) at 200°C for 30 min. Following a heat treatment at 400°C (100 Torr of H_2), the rate was measured again. The initial rate of the disappearance of undeuterated cyclopentane was corrected for physisorption and calculated by standard means (28).

5. Transmission Electron Microscopy (TEM)

A Hitachi HF-2000 high resolution analytical electron microscope equipped with a field emission cathode was used for rhodium particle size analysis. The microscope was operated at 200 keV in the bright field mode. The *ex situ* treated samples were supported on holey carbon coated copper grids.

III. RESULTS

1. Methylcyclopentane Conversion

The turnover frequencies (TOFs) at 200°C for four Rh catalysts with different proton concentrations are shown in Fig. 1. Overall, the following trend emerges: Rh/SiO_2 > Rh/$NaY_{(neutr)}$> Rh/NaY > Rh/HY. Conversions and product distributions for 5 and 30 min time on stream (TOS) are presented in Table 1. At this temperature, ring opening and deep hydrogenolysis (DH) to methane are predominant for

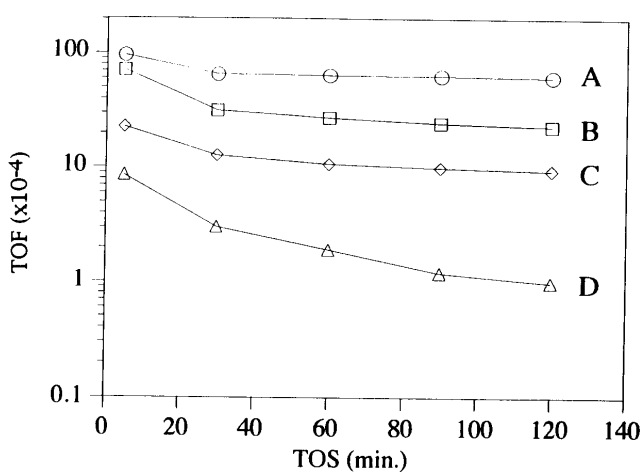

FIG. 1. The activity of (A) Rh/SiO_2, (B) $Rh/NaY_{(neutr)}$, (C) Rh/NaY, and (D) Rh/HY for MCP reaction at 200°C versus TOS.

TABLE 1

Conversion and Product Distribution of MCP Reaction at 200°C

Catalyst	Rh/HY	Rh/NaY	$Rh/NaY_{(neutr)}$ (I)	Rh/SiO_2	Phys. Mixt. (I) + HY
Conv. (%)	7.7	10.0	61.6	79.1	14.6
Total STY[a]	10.8	30.3	112.0	318.4	66.8
			Product Dist.[b] after 5 min		
Methane	23.6	18.0	9.6	7.9	9.3
Ethane	1.8	2.6	1.3	0.6	1.4
Propane	0.9	0.9	0.6	0.4	0.4
i-Butane	1.5	1.9	1.0	0.9	1.2
n-Butane	1.4	6.7	0.8	0.4	0.5
i-Pentane	5.9	1.5	5.3	4.4	4.5
n-Pentane	1.8	1.5	1.9	0.9	1.0
Cyclopentane	1.3	0.9	0.3	0.1	0.6
2-MP	35.0	40.2	44.2	56.2	44.6
3-MP	19.7	21.3	29.0	24.3	30.6
n-Hexane	4.9	5.0	6.0	4.0	5.7
Benzene	—	—	—	—	—
Cyclohexane	2.3	—	—	—	0.2
			Product Dist. after 30 min		
Methane	15.7	13.6	5.4	6.3	8.8
Ethane	—	2.2	0.6	0.3	1.3
Propane	—	0.7	0.2	0.2	0.4
i-Butane	1.0	1.6	0.5	0.7	1.1
n-Butane	1.0	0.8	0.3	0.2	0.5
i-Pentane	4.3	5.8	2.7	3.7	4.3
n-Pentane	1.2	1.2	0.7	0.6	0.8
Cyclopentane	1.4	0.9	0.5	0.1	0.7
2-MP	39.9	44.7	48.0	59.4	45.1
3-MP	23.0	23.2	36.3	26.0	30.9
n-Hexane	3.1	5.0	4.6	2.6	5.6
Benzene	—	—	—	—	—
Cyclohexane	9.4	0.3	—	—	0.7

[a] STY expressed as MCP molecules converted $\cdot$ s^{-1} $\cdot$ Rh atoms^{-1} ($\times$ 10^{-4}).
[b] Moles per 100 moles MCP converted.

all catalyst samples. Even the proton-rich Rh/HY catalyst produces less than 10% of ring enlargement, while other samples with lower proton concentration yield a negligible amount. Conversion over the neutralized catalysts $Rh/NaY_{(neutr)}$ and Rh/SiO_2 gives only RO and DH products, confirming that ring-opening hydrogenolysis is a metal-catalyzed reaction, whereas ring enlargement requires support acidity. As six molecules of methane are produced per molecule of MCP in deep hydrogenolysis, the selectivities, i.e., the fraction of converted MCP molecules leading to a given product, are shown explicitly in Table 2. The turnover frequencies at 200°C for the prevailing ring-opening reaction have been compiled in Table 3.

The catalytic signature of zeolite supported Rh differs strikingly from that of zeolite supported Pt and Pd when supported on the proton-rich HY zeolite (see Table 4). All data were taken at 5 min TOS. A reaction temperature of 250°C was used for the comparison of Rh and Pt while the data for Pd had been taken at 275°C. The data of Pd/HY and Pt/HY were published in previous papers from this laboratory (2, 7, 25). Under these conditions ring enlargement over Rh/HY (43.6%), though faster than at 200°C, is still much lower than over Pt/HY (70.1%) and Pd/HY (82.5%). Deep hydrogenolysis is faster on Rh than on the other two metals.

With longer times on stream the product distribution over Rh/HY changes significantly because methane production with the largest ensemble requirement among the competing reactions decreases strongly. This is illustrated in Fig. 2, which shows the yields (conversion $\times$ selectivities) plotted versus TOS for deep hydrogenolysis, ring opening, and ring enlargement.

2. Temperature-Programmed Oxidation (TPO)

Temperature-programmed oxidation was performed on 3% Rh/zeolite Y samples and 5% Rh/SiO_2. A small but significant amount of carbon was detected on the zeolite

TABLE 2

Turnover Frequencies, Selectivities, and Product Ratios for Rh Catalysts with Different Support Acidities at 200°C

			Selectivity (%)											
	TOF[a]		DH[b]		RO[c]		RE[d]		2MP/3MP		3MP/nHex		M_f[e]	
TOS (min)	5	30	5	30	5	30	5	30	5	30	5	30	5	30
Rh/HY	10.8	3.9	18.9	11.5	78.1	77.5	3.0	11.0	1.8	1.7	4.0	7.5	1.04	0.69
Rh/NaY	30.3	19.8	17.2	13.6	82.8	86.1	—	0.3	1.9	1.9	4.2	4.6	1.55	1.73
$RhNaY_{(neutr)}$ (I)	112	49.3	10.9	5.5	89.1	94.5	—	—	1.5	1.3	4.8	7.9	1.92	1.57
Rh/SiO_2	318	216	7.6	5.8	92.4	94.2	—	—	2.3	2.3	6.1	10.0	1.53	1.23
(I) + HY	66.8	31.6	9.4	8.7	90.4	90.6	0.2	0.7	1.5	1.5	5.4	5.5	1.77	1.70

[a] $(10^{-4}$ MCP molecules converted) · s^{-1} · exposed Rh metal $atom^{-1}$.
[b] Deep hydrogenolysis.
[c] Ring opening.
[d] Ring enlargement.
[e] Fission parameter: $M_f = \Sigma C_i(n-i)/C_1$.

supported catalysts after 2 h on stream at 200°C, whereas no carbon was detected on Rh/SiO_2 under these conditions. The TPO profiles are presented in Fig. 3 and the quantitative data are given in Table 5. The TPO profile for Rh/HY shows two peaks at 130 and 324°C, whereas Rh/NaY displays one broad peak at 307°C. The profile for $Rh/NaY_{(neutr)}$ shows two peaks at 120 and 260°C. A negative CO_2 production above 123°C of the neutralized catalyst indicates the presence of Na_2O, which reacts with CO_2 to form Na_2CO_3. It is remarkable that the amount of carbonaceous deposits on used Rh catalysts after 2 h TOS at 200°C does not show a positive correlation with the proton concentration, rather it appears that less carbonaceous deposits exist on Rh/HY than on $Rh/NaY_{(neutr)}$.

3. *Cyclopentane H/D Exchange*

H/D exchange of cyclopentane with D_2 was used to characterize the extent of metal deactivation after use as a catalyst. The initial rates of disappearance of d_0 are listed in Table 6 for the Rh/Y catalysts. After MCP conversion at 200°C the H/D exchange rate over Rh/HY decreases from 35.1 to 26.5, indicating a loss in exposed Rh atoms by only 24%. Upon treating this deactivated catalyst in H_2 at 400°C, the isotopic exchange rate increases to 34.5. In the case of Rh/NaY, only a slight decrease in the isotopic exchange rate is caused by use of the catalyst in MCP conversion. $Rh/NaY_{(neutr)}$ even appears to display a small increase in exchange rate after exposure to MCP + H_2.

TABLE 3

Initial RO Rates for Rh/Y Catalysts at 200°C

Catalyst	RO rate[a]
$Rh/NaY_{(neutr)}$	99.8
$Rh/NaY_{(neutr)}$ + HY	60.4
Rh/NaY	25.1
Rh/HY	8.4

[a] $(10^{-4}$ MCP molecules converted) · s^{-1} · exposed Rh^0 $atom^{-1}$.

IV. DISCUSSION

1. *Comparison of Rh with Pd and Pt*

Many investigations comparing the hydrogenolytic activity of Rh, Pd, and Pt catalysts for various hydrocarbon

TABLE 4

Product Distribution of Rh/HY and Pt/HY at 250°C after 5 min TOS

	Rh/HY (250)	Pt/HY (250)[a]	Pd/HY (275)[b]
Conversion (%)	8.0	24.4	26.9
	Product Dist. (%)[c]		
Methane	48.6	—	—
Ethane	1.8	—	—
Propane	1.7	1.8	1.7
i-Butane	2.3	11.5	6.1
n-Butane	2.0	1.2	1.4
i-Pentane	4.5	6.0	3.5
n-Pentane	1.5	0.9	2.4
Cyclopentane	2.4	0.3	—
2,2-Dimethylbutane	—	0.3	—
2,3-Dimethylbutane	—	0.5	—
2-Methylpentane	5.6	1.8	0.9
3-Methylpentane	4.5	1.1	0.9
n-Hexane	1.4	0.7	0.6
Benzene	1.6	8.8	29.6
Cyclohexane	22.2	61.5	52.9
$\geq C_7$	—	8.6	—

[a] Ref. (7).
[b] Ref. (2).
[c] Moles per 100 moles MCP converted.

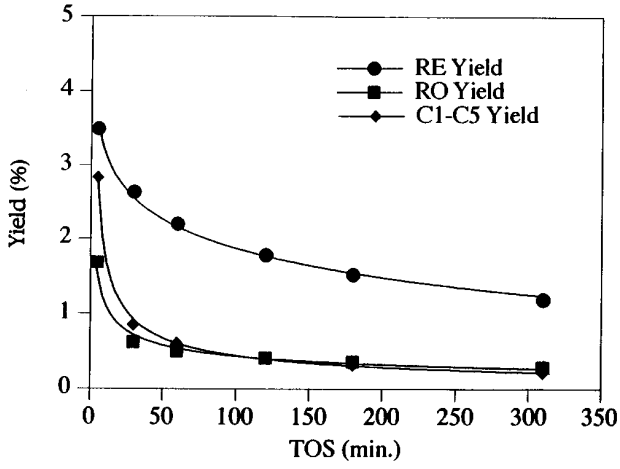

FIG. 2. Yields of RE, RO, and DH products versus TOS over 3 wt% Rh/HY at 250°C.

reactions have been reported and reviewed (29–31). This discussion will focus on the MCP activity data for zeolite Y supported Rh and will make a comparison with data reported previously in this laboratory for Pd and Pt. For Rh/HY at 200°C, RE is the minor reaction compared to RO with a selectivity of 3.0% after 5 min on stream, while at 250°C, the RE selectivity is 43.6%. The increase in RE selectivity with temperature is in accord with the higher activation energy of the RE process. Accordingly, the RE selectivity of Pt/HY and Pd/HY, which have to be tested at higher temperatures, was found to be 70.4% for Pt at 250°C and 82.5% for Pd at 275°C (after 5 min on stream). Table 4 illustrates the differences among the HY supported metals Rh, Pt, and Pd. Demethylation, RO, and RE are all prominent over Rh/HY, whereas only RE dominates over Pd/HY and Pt/HY catalysts.

The high activation energy of the RE reaction is in accordance with the most likely mechanism of this reaction (32, 33). Once a tertiary carbenium ion with the structure of the methylcyclopentane molecule is formed, it can isomerize to an ion which has a protonated cyclopropane ring fused to the C_5 ring. Opening of one C–C bond transforms this ion into a secondary ion with C_6 ring structure.

The RO selectivity of Rh/NaY does not change with TOS at 200°C, and the RE activity is very low. This catalyst was

TABLE 5

Carbon Retention during MCP Conversion

Catalyst[a]	C/Rh[b]
3% Rh/HY	1.67
3% Rh/NaY	0.76
3% Rh/NaY$_{(neutr)}$	2.94

[a] After 2 h on stream.
[b] Carbon per exposed Rh metal atom.

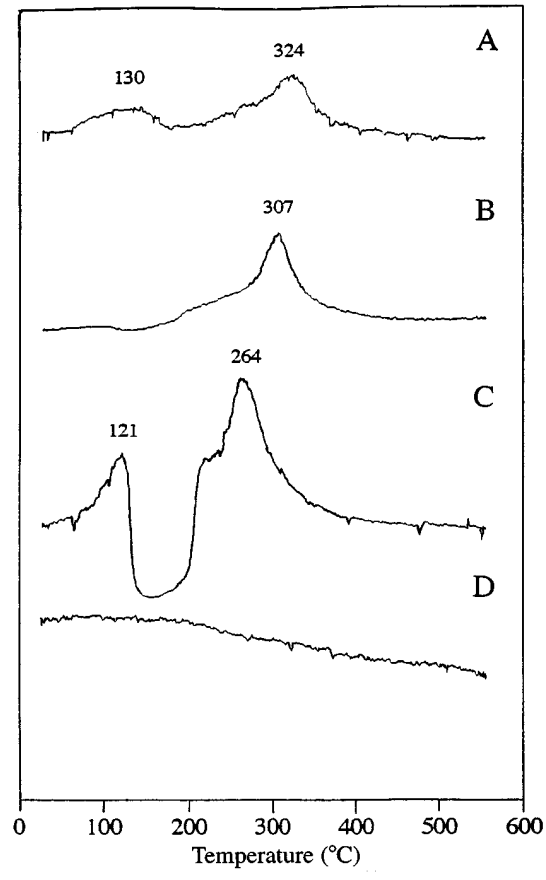

FIG. 3. CO_2 profiles obtained during TPO of catalysts after 2 h TOS of the MCP reaction (200°C). (A) 3 wt% Rh/HY, (B) 3 wt% Rh/NaY, (C) 3 wt% Rh/NaY$_{(neutr)}$, and (D) 5 wt% Rh/SiO_2.

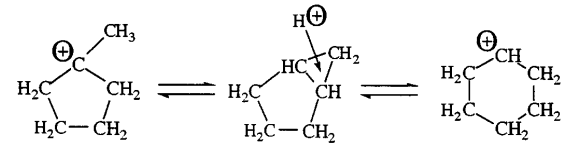

SCHEME 1

also tested at 250°C; it still displayed almost no RE activity. A similar type of behavior was observed for Pt/NaY (25). In the case of Pd/NaY, selectivity changes dramatically with TOS (2, 7). Initially high RO selectivity is observed, followed by a gradual increase in RE selectivity with TOS. These results are explained by the fact that RO hydrogenolysis is an ensemble sensitive reaction so that the number of suitable ensembles rapidly decreases due to deactivation by coke. It is interesting that the Pd/NaY selectivity shifts from RO to RE with TOS while Rh/NaY does not, even though Rh/NaY possesses a higher H^+/metal ratio after reduction.

In the absence of protons, rhodium catalyzes RO at 150–200°C confirming that rhodium is one of the most active metals for the hydrogenolysis of hydrocarbons (34). An examination of the selectivities with respect to the ring-

TABLE 6

Initial Rate of Disappearance of Undeuterated Cyclopentane (d_0)

Samples	Rate 1[a]	Rate 2	Rate 3
Rh/HY	35.1	26.5	34.5
Rh/NaY	22.0	21.1	22.1
$Rh/NaY_{(neutr)}$	34.7	35.4	38.0

[a] %/min — 10 mg at 100°C. Rate 1, after reduction at 400°C. Rate 2, after exposure to H_2 and MCP at 200°C. Rate 3, after heating to 400°C and exposure to 100 Torr of H_2.

opening products reveals some interesting features (see Table 2). The 3-methylpentane/*n*-hexane ratio should be 0.5, assuming a statistical ring-opening product distribution. In zeolites the ratio is higher. In the case of Pt it is a factor of 2 higher than statistical, which was tentatively explained by impeded roll over (35). With Pd the deviation between the experimental 3-methylpentane/*n*-hexane ratio and that predicted by statistics was a factor of 3 (2, 7). With Rh/NaY and $Rh/NaY_{(neutr)}$ this ratio becomes 4.6 and 7.9, respectively. A relative production of *n*-hexane during MCP hydrogenolysis far below the values predicted by statistics or thermodynamics has been reported by other authors using Rh with amorphous supports (36, 37). This finding cannot be ascribed to specific steric interaction with the zeolite. It rather indicates that the opening of the bond between tertiary and secondary C atoms is very specific for the metal (Pt > Pd ≫ Rh).

To gain some insight into the preferred positions of C–C bond fission, "fission parameter" (M_f) data are given in Table 2 (38, 39). A value of 1 results from terminal splitting while $M_f < 1$ corresponds to multiple splitting and $M_f > 1$ to internal fission. Initially, the M_f of Rh/HY (200°C) is 1.04 and then is lowered to 0.69 after 30 min in stream. It appears that terminal splitting initially dominates, with multiple splitting occurring later on stream. Initially deep hydrogenolysis is important on Rh, as shown in Fig. 2; but the propensity of the metal to catalyze this multiple C–C bond fission markedly decreases with reaction time. It is known that multiple C–C bond fission requires large ensembles of contiguous metal atoms, and therefore is very sensitive to even small deposits of carbonaceous overlayers (40).

2. *The Effect of Proton Concentration*

The most striking result of this study is that the catalytic activity of Rh is distinctly lowered by protons coexisting in the catalyst. This is illustrated in Fig. 1, which shows that the overall activity decreases in the order $Rh/SiO_2 > Rh/NaY_{(neutr)} > Rh/NaY > Rh/HY$. The trend for catalysts with the same microporous support clearly is that the catalytic activity *increases with decreasing support acidity*. This contrasts with the effect of protons on the activity of transition metals when tested with neopentane hydrogenolysis as the probe. In that case, activity is always found to increase with the formation of proton adducts (22).

Before evaluating these results in terms of the models described in the Introduction, more trivial causes for this trend have to be eliminated. One of these is deactivation by (hydro-) carbonaceous overlayers. The TPO data in Table 5 and Fig. 3 show that differences in coke formation among the zeolite supported Rh samples are small; moreover there appears to be more coke on $Rh/NaY_{(neutr)}$ than Rh/HY. This is in contrast to the trend observed previously with Pd, for which the data seemed to indicate that coke formation increases with support acidity (7). As mentioned, the unusual behavior of the neutralized sample, which displays a "negative CO_2 peak" is indicative of the presence of Na_2O or NaOH particles which absorb CO_2 and form Na_2CO_3.

To exclude pore diffusion control as the factor responsible for the higher activity of Rh/SiO_2 relative to the zeolite supported metals, the apparent activation energies of Rh/SiO_2 and $Rh/NaY_{(neutr)}$ were measured. According to the Wheeler model, pore diffusion control lowers the apparent activation energy ultimately to half the true activation energy (41). Activation energies for the RO reaction were determined to be 18.4 and 20.4 kcal/mol for Rh/SiO_2 and $Rh/NaY_{(neutr)}$, respectively. The values are very similar and do not support pore diffusion control in NaY. In previous work comparing Rh/NaY and Rh/SiO_2 for neopentane conversion, it was found that both catalysts possessed similar activation energies for that reaction (22).

In an effort to identify the effect of the MCP reaction on the quantity and quality of exposed metal atoms. H/D isotope exchange of cyclopentane was used to probe metal sites before and after MCP reaction. This is known to be a very site specific and sensitive technique. This results in Table 6 show that a small fraction of the metal sites present in Rh/HY are blocked after the MCP reaction, causing a drop in the initial exchange rate from 35.1 to 26.5. This indicates a decrease in the number of exposed Rh atoms by only 24.5%. Remarkably, the site blocking material can be removed by mere hydrogenation at 400°C, which restores the original exchange rate. Clearly, the carbon deposit is not graphitic coke (42), but more likely consists of chemisorbed molecules or carbenium ions. With Rh/NaY and Rh/NaY_{neutr} this test shows only a negligible change in isotope exchange rate after MCP reaction. This supports the view that on Rh/HY the adsorbed species are tertiary carbenium ions, which are absent in Rh/NaY_{neutr} and scarce in Rh/NaY.

After having eliminated carbonaceous deposits as the primary cause for the decrease in activity with increasing proton content of the zeolite, the question arises whether close proximity of protons and metal particles is essential. The data in Table 2 show that the bifunctional catalyst, Rh/HY, that contains Rh clusters and protons in the same zeolite is 2.5 times more active for ring enlargement at

200°C than a physical mixture of $Rh/NaY_{(neutr)}$ and HY with the same number of metal atoms and protons. This confirms previous findings with Pd/HY that the most active site for RE contains metal clusters and protons in each other's close proximity. In the absence of interparticle migration in the physical mixture, the average distance between metal clusters and protons is estimated to be about 4 or 5 orders of magnitude larger than in Rh/HY. For the Pd/Y system, Bai *et al*. showed that the RE rate of MCP on Pd/HY was 20 times greater than that of the physical mixture of $Pd/NaY_{(neutr)}$ and HY. It was therefore proposed that the RE reaction of MCP was catalyzed by $[Pd_nH_x]^{x+}$ adducts, rather than by separate metal and acid sites (2). Previously, Chow *et al*. compared Pt/HY with a physical mixture of Pt/SiO_2 and HY for this reaction at 250°C (25). For these bifunctional Pt containing catalysts, ring enlargement was the predominant process, and the RE rates differed by a factor of 1.2. This small difference between physical mixture and bifunctional zeolite supported catalyst could be partly due to lower transport resistance of SiO_2 supported metals, in particular after intergranular ion migration.

In Rh/NaY and Rh/HY, an equilibrium (21) is established:

$$Rh^0 + H^+ \leftrightarrows Rh^+ + 1/2\ H_2. \qquad [1]$$

Some Rh^+ is present after reduction; its amount will not increase with TOS because of the hydrogen-rich atmosphere during the reaction. Deactivation can, therefore, not be ascribed to an increase in Rh^+ concentration. So simple coking of the catalyst and oxidation of Rh^0 to Rh^+ are ruled out as possible causes for the observed activity trend of the catalysts.

The influence of the metal particle size on catalytic activity must also be addressed. The Rh particle sizes in Rh/SiO_2 and $Rh/NaY_{(neutr)}$ as determined by TEM are ~40 and ~15 Å, respectively. The particle sizes of Rh/HY (<10 Å) and Rh/NaY (10–15 Å) are based on data from TEM and EXAFS (21). Ponec *et al*. have shown that the smallest particles display the lowest hydrogenolytic activity for catalysts containing Ni, Ir, or Pt (37). Later work by Ponec, using Ni/SiO_2 catalysts, revealed that under mild conditions (200–280°C), where carbonaceous layer deposition was minimal, small Ni particles (10 Å) are less active in MCP hydrogenolysis than large particles (60 Å). The differences are most pronounced at low temperature (38).

The present results confirm the trend found for all other zeolite supported transition metals that metal dispersion is higher on acid zeolites because of the well-known anchoring effect of protons. As hydrogenolysis has often been found to have a high ensemble requirement, the low activity of the sample with highest metal dispersion could be a simple particle size effect. However, this hypothesis is rejected on the basis of the totality of the data obtained by Dalla Betta and Boudart (10) and by the present group (9, 22) that interaction of transition metal clusters with acid sites in zeolites always leads to electron deficiency, usually resulting in enhanced catalytic activity. Seen in this light, the low catalytic activity of electron-deficient Rh in HY is an anomaly. It can, however, be rationalized by considering that Rh permits probing of such catalysts at lower temperature than is possible with Pt or Pd. Whenever the reaction temperature enables adsorbed carbenium ions to reach the transition state for RE, this reaction is observed; only with Rh can catalysis be studied at such low temperature that adsorbed carbenium ions are unable to react further. Here the unique situation is encountered where an adsorbed carbenium ion merely blocks a metal site.

3. Metal Site Blocking

In the Introduction it was argued that the model (b), assuming formation of Rh–proton adducts, predicts that carbenium ions will block metal sites so that the rate of purely metal-catalyzed RO reactions will be significantly lower than on a monofunctional catalyst at the same temperature. The data in Table 3 agree with this model as the RO rate decreases with proton concentration. The RO rate over $Rh/NaY_{(neutr)}$ is more than an order of magnitude greater than over Rh/HY. In the case of Rh/HY, this reduction in RO rate is observed with only little additional RE activity. The RO rate of $Rh/NaY_{(neutr)}$ is also ~40% greater than that of the physical mixture of $Rh/NaY_{(neutr)}$ + HY. This difference is likely a result of some carbenium ion migration from acidic sites to the metal sites.

The results thus confirm that metal–proton adducts act as hybrid sites; chemisorption of an alkane can occur in two ways:

(i) $C_nH_m \Rightarrow C_nH_{m-1,ads} + H_{ads}$
(ii) $C_nH_m + H^+_{adduct} \Rightarrow (C_nH_{m-1})^+_{ads} + H_2$.

The adsorption complex (i) is the first intermediate in ring opening and deep hydrogenolysis; adsorption complex (ii) can lead to MCP ring enlargement, if temperature permits, to overcome the activation barrier for that process. If the temperature is too low for this, the complex simply is a competitor for adsorption (i).

V. CONCLUSIONS

The activity of zeolite supported Rh for MCP conversion decreases with increasing proton concentration of the support: $Rh/SiO_2 > Rh/NaY_{(neutr)} > Rh/NaY > Rh/HY$. This trend is opposite to that expected for the electron deficiency of metal particles and the activity sequence observed for neopentane conversion on such catalysts. The trend found with MCP is not matched by the extent of formation of carbonaceous overlayers, which is low for these catalysts and highest for $Rh/NaY_{(neutr)}$. The facile removal of such deposits by a H_2 treatment at 400°C further shows that these overlayers are certainly not "hard coke," but rather

chemisorbed molecules. Identification of the fraction of exposed metal sites after MCP treatment by an isotope exchange reaction shows that in the presence of protons 75% of the metal sites remain exposed whereas 25% are covered, presumably with tertiary carbenium ions $C_5H_{11}^+$.

At 200°C, rhodium is a very efficient hydrogenolysis catalyst; ring opening is the dominating reaction on all Rh/Y samples and deep hydrogenolysis is significant. Ring enlargement, though being a minor contributor, is still 2.5 times faster on Rh/HY than on a physical mixture of Rh/$NaY_{(neutr)}$ and HY with the same number of metal atoms and protons. This confirms that the most active RE sites contain metal clusters and protons in each other's close proximity, presumably forming Rh–proton adducts. However, as a consequence of the high activation energy for ring enlargement, the majority of carbenium ions that are adsorbed on Rh–proton adducts do not react further at 200°C. They simply block part of the Rh surface and lower the propensity of the metal to catalyze the ring opening of MCP.

ACKNOWLEDGMENTS

The authors gratefully acknowledge financial support from the National Science Foundation, Contract CTS-9221841. The rhodium ($RhCl_3$) was obtained from Johnson/Matthey through their Precious Metals Loan Program. We wish to thank Professor Vinayak Dravid, Department of Material Science, Northwestern University, for use of the Hitachi HF-2000 electron microscope.

REFERENCES

1. Mills, G. A., Heinemann, H., Millikan, T. H., and Oblad, A. G., *Ind. Eng. Chem.* **45**, 134 (1953).
2. Bai, X., and Sachtler, W. M. H., *J. Catal.* **129**, 121 (1991).
3. Lei, G., and Sachtler, W. M. H., *J. Catal.* **140**, 601 (1992).
4. Carvill, B. T., Lerner, B. A., Lei, G., Zholobenko, V., and Sachtler, W. M. H., "Preprints ACS Petroleum Division Symposium, New Catalytic Chemistry Using Molecular Sieves, Chicago." Am. Chem. Soc., Washington, DC, 1993.
5. Zholobenko, V. L., Lei, G., Carvill, B. T., Lerner, B. A., and Sachtler, W. M. H., *J. Chem. Soc. Faraday Trans.* **90**, 233 (1994).
6. Xu, L., Zhang, Z., and Sachtler, W. M. H., *J. Chem. Soc. Faraday Trans.* **88**, 2291 (1992).
7. Homeyer, S. T., Karpiński, Z., and Sachtler, W. M. H., *J. Catal.* **123**, 60 (1990).
8. Karpiński, Z., Homeyer, S. T., and Sachtler, W. M. H., *in* "Structure-Activity Relationships in Heterogeneous Catalysis" (R. K. Grasselli and A. Sleight, Eds.), Studies in Surface Science and Catalysis, Vol. 67, p. 203. Elsevier, Amsterdam, 1991.
9. Sachtler, W. M. H., and Stakheev, A. Yu., *Catal. Today* **12**, 283 (1992).
10. Dalla Betta, R. A., and Boudart, M., *in* "Proceedings, 5th International Congress on Catalysis, Palm Beach, 1972" (J. W. Hightower, Ed.) p. 1329. North-Holland, Amsterdam, 1973.
11. Boudart, M., Aldag, A. W., Ptak, L. D., and Benson, J. E., *J. Catal.* **11**, 35 (1968).
12. Besoukhanova, C., Guidot, J., and Barthomeuf, D., *J. Chem. Soc. Faraday Trans. 1* **77**, 1595 (1981).
13. Larsen, G., and Haller, G. L., *Catal. Lett.* **3**, 103 (1989).
14. Jiang, X., Gao, Z. N., Ruan, Z. K., Sheng, S. S., Huang, J. S., Luo, X. H., and Xu, Y. X., *in* "Symposium on Chemically Modified Molecular Sieves, 206th National Meeting, American Chemical Society, Chicago, 1993" p. 555. Am. Chem. Soc., Washington, DC, 1993.
15. Wehman-Ooyevaar, I. C. M., Grove, D. M., de Vaal, P., Dedieu, A., and Koten, G., *Inorg. Chem.* **31**, 5484 (1992).
16. Kazarian, S. G., Hamley, P. A., and Poliakoff, M., *J. Am. Chem. Soc.* **115**, 9069 (1993).
17. Yates, D. J. C., and Sinfelt, J. H., *J. Catal.* **8**, 348 (1967).
18. Boudart, M., and Ptak, L. D., *J. Catal.* **16**, 90 (1970).
19. Coq, B., Dutartre, R., Figueras, F., and Tazi, T., *J. Catal.* **122**, 438 (1990).
20. Yao, H. C., and Shelef, M., *J. Catal.* **56**, 12 (1979).
21. Tomczak, D. C., Schünemann, V., Lei, G. D., Treviño, H., and Sachtler, W. M. H., *Microporous Mater.* **5**, 263 (1996).
22. Wong, T. T. T., and Sachtler, W. M. H., *J. Catal.* **141**, 407 (1993).
23. Osborn, J. A., Thomas, K., and Wilkinson, G., *in* "Inorganic Syntheses" (F. A. Cotton, Ed.), Vol. 13, p. 213. McGraw-Hill, New York, 1973.
24. Karpiński, Z., Butt, J. B., and Sachtler, W. M. H., *J. Catal.* **119**, 521 (1989).
25. Chow, M., Park, S. H., and Sachtler, W. M. H., *Appl. Catal.* **19**, 349 (1985).
26. Augustine, S. M., Alameddin, G. N., and Sachtler, W. M. H., *J. Catal.* **115**, 217 (1989).
27. Augustine, S. M., and Sachtler, W. M. H., *J. Catal.* **106**, 417 (1987).
28. Kemball, C., *Adv. Catal.* **11**, 223 (1959).
29. Gault, F. G., *Adv. Catal.* **30**, 1 (1981).
30. Sinfelt, J. H., *Adv. Catal.* **23**, 91 (1973).
31. Kemball, C., *Catal. Rev.* **5**, 33 (1971).
32. Brouwer, D. M., and Hoogeveen, H., *Progr. Phys. Org. Chem.* **9**, 179 (1972).
33. Brouwer, D. M., *in* "Chemistry and Chemical Engineering of Catalytic Processes" (R. Prins and G. C. A. Schuit, Eds.), p. 173. Sijthoff & Noordhof, Alphen a.d. Rijn, 1980.
34. Anderson, J. R., and Baker, B. G., *Proc. R. Soc. London A* **271**, 402 (1963).
35. Moretti, G., and Sachtler, W. M. H., *J. Catal.* **116**, 350 (1989).
36. Schepers, F. J., Van Senden, J. G., Van Broekhoven, E. H., and Ponec, V., *J. Catal.* **94**, 400 (1985).
37. Anderson, J. B. F., Burch, R., and Cairns, J. A., *J. Chem. Soc. Faraday Trans. 1* **83**, 913 (1987).
38. Matsumoto, H., Saito, Y., and Yoneda, Y., *J. Catal.* **19**, 101 (1970).
39. Van Schaik, J. Rl. H., Dessing, R. P., and Ponec, V., *J. Catal.* **38**, 273 (1975).
40. Sachtler, W. M. H., and van Santen, R. A., *in* "Advances in Catalysis" (D. D. Eley, H. Pines, and P. B. Weisz, Eds.), Vol. 26, p. 69. Academic Press, New York, 1977.
41. Wheeler, A., *Adv. Catal.* **3**, 249 (1954).
42. McCarty, J. G., and Wise, H. J., *J. Catal.* **116**, 350 (1989).
43. Van Broekhoven, E. H., Schoonhoven, J. W. F., and Ponec, V., *Surf. Sci.* **156**, 889 (1985); *in* "Proceedings, 3rd Symposium on Small Particles and Inorganic Clusters, Berlin, 1984."
44. Schepers, F. J., Van Broekhoven, E. H., and Ponec, V., *J. Catal.* **96**, 82 (1985).